BJCP British Journal of Clinical Pharmacology

DOI:10.1111/bcp.12639

# Population pharmacokinetics of dolutegravir in HIV-infected treatment-naive patients

**Jianping Zhang,[1] Siobhán Hayes,[2] Brian M. Sadler,[2] Ilisse Minto,[3] Julie Brandt,[3] Steve Piscitelli,[1] Sherene Min[3] & Ivy H. Song[1]**

*[1]Clinical Pharmacology, GlaxoSmithKline, Research Triangle Park, NC, USA, [2]ICON, Marlow, UK and [3]GlaxoSmithKline, Research Triangle Park, NC, USA*

**Correspondence**
Dr Ivy H. Song, Clinical Pharmacology, GlaxoSmithKline, 5 Moore Drive, Research Triangle Park, NC 27709, USA.
Tel.: +1 919 483 7197
E-mail: ivy.h.song@gsk.com

**Keywords**
dolutegravir, integrase inhibitor, population pharmacokinetics, treatment-naive

**Received**
2 October 2014

**Accepted**
22 March 2015

**Accepted Article Published Online**
27 March 2015

## WHAT IS ALREADY KNOWN ABOUT THIS SUBJECT

- Dolutegravir is an HIV integrase strand transfer inhibitor that has been developed for the treatment of HIV infection.
- The pharmacokinetics of dolutegravir have been characterized in healthy volunteers and treatment-naive, HIV-1 infected adult patients.

## WHAT THIS STUDY ADDS

- This article is the first description of the population pharmacokinetics of dolutegravir in treatment-naive, HIV-1 infected adult patients. The influence of patient covariates on the exposure of dolutegravir has been explored.

## AIM

Dolutegravir is the newest integrase inhibitor approved for HIV treatment and has demonstrated potent antiviral activity in patient populations with a broad range of treatment experience. This analysis aimed to characterize the population pharmacokinetics of dolutegravir in treatment-naive patients and to evaluate the influence of patient covariates.

## METHODS

A population pharmacokinetic model was developed using a non-linear mixed effect modelling approach based on data from 563 HIV-infected, treatment-naive adult patients in three phase 2/3 trials who received dolutegravir (ranging from 10–50 mg once daily) alone or in combination with abacavir/lamivudine or tenofovir/emtricitabine.

## RESULTS

The pharmacokinetics of dolutegravir were adequately described by a linear one compartment model with first order absorption, absorption lag time and first order elimination. Population estimates for apparent clearance, apparent volume of distribution, absorption rate constant and absorption lag time were 0.901 l $h^{-1}$, 17.4 l, 2.24 $h^{-1}$, and 0.263 h, respectively. Weight, smoking status, age and total bilirubin were predictors of clearance, weight was a predictor of volume of distribution and gender was a predictor of bioavailability. However, the magnitude of the effects of these covariates on steady-state dolutegravir plasma exposure was relatively small (<32%) and was not considered clinically significant. Race/ethnicity, HBV/HCV co-infection, CDC classification, albumin, creatinine clearance, alanine aminotransferase or aspartate aminotransferase did not influence the pharmacokinetics of dolutegravir in this analysis.

## CONCLUSIONS

A population model that adequately characterizes dolutegravir pharmacokinetics has been developed. No dolutegravir dose adjustment by patient covariates is necessary in HIV-infected treatment-naive patients.

## Introduction

Dolutegravir (DTG; Tivicay®, ViiV Healthcare, Research Triangle Park, NC, USA) is an HIV integrase strand transfer inhibitor (INSTI) that has been approved by the Food and Drug Administration (FDA) and the European Medicines Agency (EMA) for the treatment of HIV infection in a broad patient population [1, 2]. Phase 3 studies in treatment-naive and treatment-experienced subjects demonstrated that DTG has sustained antiviral activity and desirable safety profiles in combination with various background therapies in HIV-infected adults [3, 4]. Furthermore, *in vitro* experiments suggest that DTG retains activity against viral strains harboring major integrase resistance mutations selected for by both raltegravir (RAL) and elvitegravir (EVG) [5], two previously approved integrase inhibitors. These findings have been confirmed in clinical studies demonstrating DTG's activity in subjects with resistance to RAL [6].

The pharmacokinetics (PK) of DTG have been evaluated in both healthy and HIV-1 infected adult subjects. The primary objectives of evaluating DTG PK in healthy subjects were to understand the disposition of DTG after oral administration and to assess the effect of formulations, food, drug–drug interactions and enzyme polymorphisms on DTG PK. Effects of intrinsic factors, including age, gender, body size, and race/ethnicity and extrinsic factors, including smoking, hepatitis B virus/hepatitis C virus (HBV/HCV) co-infection and disease status, were primarily evaluated in HIV-infected subjects using sparse PK samples collected in phase 2/3 trials and a population PK modelling approach.

Based on *in vitro* studies and phase 1 studies, DTG is highly bound (≥98.9%) to human plasma proteins, is eliminated primarily through hepatic metabolism with minimal renal excretion (<1% of dose administered orally), is metabolized primarily through uridine diphosphate glucuronosyltransferase (UGT) 1A1 with some contribution from cytochrome P450 (CYP) 3A4, and is a substrate of P-glycoprotein (Pgp) and breast cancer resistance protein (BCRP) [1, 2]. DTG has demonstrated low to moderate between subject and within subject PK variability. In phase 1 studies in healthy subjects, between-subject variability (%BSV) for area under the plasma concentration–time curve (AUC) and maximum plasma concentration ($C_{max}$) ranged from ~20% to 40%, and for concentration at the end of the dosing interval ($C_{\tau}$) from 30% to 65%. The variability seemed higher in HIV-infected subjects than healthy subjects.

The current population PK analysis combines the data from clinical trials in treatment-naive populations from a proof-of-concept study (ING111521[7]), a phase 2b study (SPRING-1 [8]) and a phase 3 study (SPRING-2 [3]). The aims of the analysis were to build a population PK model of DTG following once daily oral administration in HIV-infected treatment-naive patients, to identify co-factors that contribute to inter-individual variability (IIV) and to assess inter-occasion variability (IOV) in DTG PK. This model was subsequently used to explore the PK/pharmacodynamic (PD) relationship between DTG exposure and efficacy/safety endpoints.

## Methods

### *Study design, dosing regimens and subjects*

The population analysis was conducted using data from three studies primarily in HIV-1 infected antiretroviral (ART) treatment-naive adults. The number of subjects, doses, and populations for each study are presented in Table 1.

Study ING111521 was a phase 2a, multicentre, randomized, parallel, double-blind, dose-ranging, placebo-controlled study to compare antiviral effect, safety, tolerability and PK of DTG monotherapy *vs.* placebo over 10 days in treatment-naive and/or treatment-experienced INSTI-naive HIV-1 infected adults who were not currently receiving antiretroviral therapy. Eligible HIV-1 infected subjects were randomized to receive one of three blinded treatments (2 mg, 10 mg or 50 mg every 24 h) or placebo for 10 days. Data for the 2 mg dose (2 × 1mg tablets) were not included in the population PK analysis as this dose has been previously shown to have different PK to higher doses and is not intended for commercial use. SPRING-1 was a phase 2b randomized, multicentre, parallel group, dose ranging study conducted in HIV-1 infected treatment-naive adults. Subjects were randomized 1: 1: 1: 1 to one of three DTG doses (10 mg, 25 mg or 50 mg once daily) or a control regimen containing efavirenz (EFV). The background nucleoside reverse transcriptase inhibitors (NRTIs) co-administered with DTG or EFV were selected by investigators and were either abacavir/lamivudine (ABC/3TC) or tenofovir/emtricitabine (TDF/FTC) fixed dose combination (FDC) tablets. SPRING-2 was a phase 3 randomized, double-blind, double-dummy, active-controlled, multicentre, parallel group, fully-powered non-inferiority study conducted in HIV-1 infected treatment-naive adults. Subjects were randomized 1: 1 to receive DTG 50 mg once daily or RAL 400 mg twice daily, both in combination with investigator-selected fixed-dose dual NRTI therapy (either ABC/3TC or TDF/FTC).

All protocols and consent forms were reviewed and approved by the institutional review boards (IRB) or ethics committees for each of the study sites, and all subjects provided signed consent. All studies were conducted in accordance with the ethical standards of the Declaration of Helsinki and its amendments, consistent with good clinical practices and local regulatory requirements.

### *Pharmacokinetic sampling*

PK sampling times for each study are presented in Table 1. Briefly, in study ING111521, serial PK samples were collected on days 1 and 10. In addition, pre-dose

**Table 1**

Overview of clinical trials included in dolutegravir population PK analysis

| Study/Phase | Population | *n* | Dose/Treatment duration | Planned PK data |
|---|---|---|---|---|
| **ING111521 (Proof of concept)** | Treatment-naive or treatment-experienced (integrase inhibitor naive) HIV-infected patients, not currently receiving antiretroviral therapy | 19 | 2, 10 and 50 mg once daily orally (data for the 2 mg dose were not included in this population PK analysis as this dose has been previously shown to have different PK to higher doses and there is no intention to commercialize the 1 mg tablet)<br>10 days | Days 1 and 10 at pre-dose, 0.5, 1, 1.5, 2, 3, 4, 6, 8, 12 and 24 h post-dose<br>Days 3, 4, 7, 8 and 9 at pre-dose |
| **SPRING-1 (Phase 2b)** | HIV-infected treatment-naive patients | 141 | 10, 25 and 50 mg DTG once daily orally with either ABC/3TC (600 mg/300 mg) or TDF/FTC (300 mg/200 mg) fixed-dose combination (FDC)<br>96 weeks | Intensive PK ($n = 45$): Week 2 at pre-dose, 2, 3, 4, 8 and 24 h post-dose; Week 12 and 24 at pre-dose and 2–4 h post-dose<br>Limited PK ($n = 96$): Weeks 2, 12, and 24 at pre-dose and 2–4 h post-dose |
| **SPRING-2 (Phase 3)** | HIV-infected treatment-naive patients | 403 | 50 mg DTG once daily with either ABC/3TC (600 mg/300 mg) or TDF/FTC (300 mg/200 mg) fixed-dose combination (FDC)<br>96 weeks | Week 4: pre-dose and 1–3 h or 4–12 h post-dose;<br>Week 24: pre-dose;<br>Week 48: pre-dose and 1–3 h or 4–12 h post-dose |

ABC, abacavir; DTG, dolutegravir; FTC, emtricitabine; PK, pharmacokinetics; 3TC, lamivudine; TDF, tenofovir disoproxil fumarate.

PK samples were collected on days 3, 4, 7, 8 and 9. In SPRING-1, serial PK samples at week 2 were collected in a subgroup of subjects receiving DTG treatment ($n = 15$ per DTG dose arm). Sparse PK samples at weeks 2, 12 and 24 were collected in most subjects receiving DTG. In SPRING-2, sparse PK samples at weeks 4, 24 and 48 were collected in most subjects receiving DTG.

## *Bioanalytical methods*

Plasma samples were analyzed for DTG using a validated analytical method [9]. DTG was extracted from human plasma by protein precipitation using acetonitrile containing [$^{15}$N $^{2}H_7$]-DTG as an internal standard. Extracts were analyzed by liquid chromatography–tandem mass spectroscopy using a TurboIonSpray® (AB Sciex, Framingham, MA, USA) interface with positive ion multiple reaction monitoring. The lower limit of the assay was 5 ng ml$^{-1}$ or 20 ng ml$^{-1}$ depending on the study, with a within- and between- run precision of ≤8.0% and ≤7.5%, respectively.

## *Population pharmacokinetic modelling*

The population PK models were developed via a non-linear mixed effects modelling approach using the first order conditional estimation method with interaction (FOCEI) of NONMEM software (version VII Level 1.2) [10]. Structural model selection was driven by the data and was based on evaluation of goodness-of-fit plots (observed *vs*. predicted concentrations, weighted residuals *vs*. predicted values or time, histograms of individual random effects etc.), successful convergence, plausibility and precision of parameter estimates and the minimum objective function value (OFV).

The population PK model of DTG was developed with 3357 plasma concentrations from 563 subjects. Records with concentrations below the limit of quantification (BLQ) represented a very small percentage of the data (1%) and were excluded from the analysis. Various models were considered and tested to describe the absorption/disposition kinetics of DTG.

Distributions of inter-individual random effects were assumed to be log-normal and were described by an exponential error model. The residual errors were described by a combined additive and proportional model. IOV was also investigated and distributions of IOV were assumed to be normal. The occasion in this analysis was defined by PK sampling week, except for study ING111521, in which day 1 through day 10 were treated as a single occasion. The inclusion of IOV in the model was based on OFV, individual predictions and the extent of IOV (CV%) relative to IIV.

Investigation of covariate–parameter relationships was based on the range of covariate values in the data set, scientific interest, mechanistic plausibility and

exploratory graphics. The covariates evaluated are identified in Table 2. A full model approach [11, 12] was implemented, where all covariate–parameter relationships of interest were entered in the model and parameters were estimated. Insignificant or poorly estimated covariates (less than 10.83 point increase of OFV for one parameter, and/or confidence intervals (CI) including the null value and/or high relative standard error (RSE >50%)) were then excluded from the model during the backward elimination process. The full model did not simultaneously include highly correlated covariates, such as body weight *vs.* body mass index (BMI) or gender *vs.* body weight. Therefore

## Table 2

Subject characteristics and demographics by study

| Covariate | Statistic or category | ING111521 | SPRING-1 | SPRING-2 | All studies |
|---|---|---|---|---|---|
| **Total number** | | **19** | **141** | **403** | **563** |
| **Age (years) at baseline** | Median [min–max] | 40 [22–53] | 35 [20–64] | 37 [18–68] | 37 [18–68] |
| **Weight (kg) at baseline** | Median [min–max] | 78.1 [60.5–106] | 76.4 [49–120] | 74.0 [39.0–135]* | 74.5 [39.0–135]* |
| **Body mass index (kg $m^{-2}$) at baseline** | Median [min–max] | 25.5 [21.7–32.7] | 24.3 [17.6–38.7] | 24.1 [14.7–47.9]* | 24.2 [14.7–47.9]* |
| **Body surface area ($m^2$) at baseline** | Median [min–max] | 1.95 [1.68–2.33] | 1.94 [1.46–2.49] | 1.90 [1.27–2.69]* | 1.92 [1.27–2.69]* |
| **Total bilirubin (μmol $l^{-1}$) at baseline** | Median [min–max] | 8.55 [5.13–18.8] | 10.0 [4.00–38.0] | 9.00 [3.00–31.0] | 9.00 [3.00–38.0] |
| **Albumin (g $l^{-1}$) at baseline** | Median [min–max] | 42.0 [38.0–47.0] | 44.0 [34.0–51.0] | 45.0 [30.0–54.0] | 45.0 [30.0–54.0] |
| **Aspartate aminotransferase (IU $l^{-1}$) at baseline** | Median [min–max] | 25.0 [15.0–42.0] | 24.0 [11.0–180] | 24.0 [12.0–133] | 24.0 [11.0–180] |
| **Alanine aminotransferase (IU $l^{-1}$) at baseline** | Median [min–max] | 22.0 [12.0–41.0] | 20.0 [8.00–260] | 21.0 [5.00–158] | 21.0 [5.00–260] |
| **Creatinine clearance (ml $min^{-1}$) at baseline** | Median [min–max] | 119 [86.0–190] | 116 [54.6–231] | 123 [64.4–239] | 121 [54.6–239] |
| **Gender, *n* (%)** | Male | 19 (100) | 122 (87) | 340 (84) | 481 (85) |
| | Female | 0 (0) | 19 (13) | 63 (16) | 82 (15) |
| **Race, *n* (%)** | Caucasian | 16 (84) | 113 (80) | 341 (85) | 470 (83) |
| | Black | 3 (16) | 16 (11) | 47 (12) | 66 (12) |
| | Asian | 0 (0) | 0 (0) | 6 (1) | 6 (1) |
| | Other | 0 (0) | 12 (9) | 9 (2) | 21 (4) |
| **Ethnicity, *n* (%)** | Non-Hispanic or Latino | 18 (95) | 118 (84) | 361 (90) | 497 (88) |
| | Hispanic or Latino | 1 (5) | 23 (16) | 42 (10) | 66 (12) |
| **Smoking, *n* (%)** | Never | 0 (0) | 72 (51) | 163 (40) | 235 (42) |
| | Current | 0 (0) | 54 (38) | 182 (45) | 236 (42) |
| | Former | 0 (0) | 15 (11) | 58 (14) | 73 (13) |
| | Unknown | 19 (100) | 0 (0) | 0 (0) | 19 (3) |
| **HCV co-infection at baseline, *n* (%)** | No | 19 (100) | 129 (91) | 359 (89) | 507 (90) |
| | Yes | 0 (0) | 11 (8) | 41 (10) | 52 (9) |
| | Unknown | 0 (0) | 1 (1) | 3 (1) | 4 (1) |
| **HBV co-infection at baseline, *n* (%)** | No | 19 (100) | 140 (99) | 396 (98) | 555 (99) |
| | Yes | 0 (0) | 1 (1) | 7 (2) | 8 (1) |
| **CDC classification of HIV infection at baseline, *n* (%)** | A | 17 (89) | 120 (85) | 353 (88) | 490 (87) |
| | B | 1 (5) | 20 (14) | 41 (10) | 62 (11) |
| | C | 1 (5) | 1 (1) | 9 (2) | 11 (2) |
| **Metal-cation containing products†, *n* (%)** | No | 19 (100) | 124 (88) | 366 (91) | 509 (90) |
| | Yes | 0 (0) | 17 (12) | 37 (9) | 54 (10) |
| **Formulation, *n* (%)** | AL | 19 (100) | 49 (35) | 0 (0) | 68 (12) |
| | AP | 0 (0) | 92 (65) | 0 (0) | 92 (16) |
| | AW | 0 (0) | 0 (0) | 403 (100) | 403 (72) |
| **Dose (mg), *n* (%)** | 10 | 9 (47) | 49 (35) | 0 (0) | 58 (10) |
| | 25 | 0 (0) | 46 (33) | 0 (0) | 46 (8) |
| | 50 | 10 (53) | 46 (33) | 403 (100) | 459 (82) |
| **Total number of samples, *n* (%)** | | 493 (15) | 985 (29) | 1879 (56) | 3357 |

CDC, Centres for Disease Control and Prevention; CYP, cytochrome P450; HBV, hepatitis B virus; HCV, hepatitis C virus; PGP, P-glycoprotein, UGT, uridine diphosphate glucuronosyltransferase.*Imputed values included in summary statistics.†Use of metal cation containing products was the only concomitant medication group involving 10% or more of the population. The number of subjects taking other concomitant medications (*Ginkgo biloba*, CYP34A inhibitors/inducers, PGP inhibitors/inducers, UGT1A1 inhibitors/inducers and UGT1A3 inhibitors/inducers) of interest was 3% or less apart from UGT1A1 inhibitors where 6% of patients were taking this concomitant medication. No subjects were taking moderate to strong CYP3A4 or PGP inducers.

several semi-final models (with one of the competing correlated covariates) were investigated. For continuous covariates, a power function was utilized. For categorical covariates, the fractional change in the typical parameter value was determined.

### Model evaluation

A prediction corrected visual predictive check [13] (PC-VPC) was performed for the final PK model. Five hundred data sets were simulated using the final model parameters, covariates, sampling times and dosing histories. Both the observed and the model predicted individual concentration values were normalized by the population prediction of the same time point. Non-parametric bootstrap analysis was also performed by generating 1000 data sets through random sampling with replacement from the original data using the individual as the sampling unit. No stratification was implemented during the random sampling. Population parameters of the final model for each data set were estimated using NONMEM and empirical 95% CIs were constructed.

### Individual predicted pharmacokinetic parameters

The final model was used to compute individual estimates of steady-state AUC(0-τ), $C_{max}$, $t_{max}$ (time to $C_{max}$) and $C_\tau$ for all subjects included in the population PK analysis following repeat dosing of the actual DTG dose administered to each subject in the study. The individual estimates of all model parameters were obtained from the final model by an empirical Bayes estimation method. Individual estimates of AUC(0-τ) were obtained as AUC(0-τ) = Dose/([CL/$F_i$]/$F$), where Dose was the actual dose administered to each subject in study, CL/$F_i$ was the individual estimate of oral clearance and $F$ was the estimated oral bioavailability in subpopulations identified by the model relative to the reference population. Individual estimates of $C_{max}$, $t_{max}$ and $C_\tau$ were obtained by simulation of the concentration–time profiles following a steady-state dose for all individuals using their individual parameter values assuming no IOV and zero values for residual variability. Summary statistics for parameter estimates were computed.

### Simulation

A simulation was performed to predict the impact of covariates on DTG exposure. The final PK model was used to simulate plasma PK profiles for the treatment-naive population following a steady-state once daily dose of 50 mg DTG. The PK parameters AUC(0-τ), $C_{max}$, $t_{max}$ and $C_\tau$ were summarized by covariate categories. Forest plots [14–16] were created for comparison of steady-state $C_{max}$, AUC(0-τ) and $C_\tau$ among various subpopulations. In this analysis, each PK parameter was first averaged by covariate categories of interest and normalized by the average of reference categories in order to express the results as the PK parameter fold change for a given covariate category from the reference category. These PK parameter fold changes were then summarized from 100 simulations to obtain the median and the corresponding 90% CI.

### Exploratory PK–PD relationship

An exploratory graphical analysis of potential exposure–response relationships was performed using individual predicted DTG exposure (steady-state $C_\tau$, $C_{max}$ and AUC(0-τ)) obtained from the final population PK model with actual doses administered in each study assuming no IOV. The following efficacy endpoints were explored: plasma HIV-1 RNA $<$50 copies ml$^{-1}$ at week 48 using the missing, switch or discontinuation equals failure (MSDF) algorithm (categorical variable) (SPRING-2 only), protocol-defined virological failure (PDVF) at week 48 (categorical variable) (SPRING-1 only); CD4+ cell count change from baseline both at week 48 and maximal change over 48 weeks (continuous variable) (SPRING-1 and SPRING-2 combined and SPRING-2 alone). The following safety endpoints were explored: change from baseline in serum creatinine concentration, creatinine clearance (CRCL), urine albumin: creatinine ratio, alanine aminotransferase (ALT), and total bilirubin (maximal change over 48 weeks and change at week 48 visit [continuous variable]); presence of the top three most common adverse events (AEs) including nausea, diarrhoea and headache (categorical variable), for both SPRING-1 and SPRING-2 combined apart from urine albumin: creatinine ratio which was not collected before week 48 in SPRING-1, and consequently was only explored for SPRING-2.

## Results

### Data, demographics, and baseline characteristics

The basic distribution of covariates and number of concentrations by study are described in Table 2.

### Population PK analysis

The PK of DTG following oral administration were adequately described by a one compartment model with absorption lag time ($t_{lag}$) and first order absorption and elimination as the final base model, with IIV in apparent clearance (CL/$F$), apparent volume of distribution ($V/F$), and first order absorption rate ($k_a$), correlation between CL/$F$ and $V/F$, IOV on CL/$F$, weight on CL/$F$ and $V/F$, increase in CL/$F$ for study ING111521, and increase in bioavailability ($F$) for the 10 mg dose. No improvement was found with the two compartment model and the additive residual error was not significant. Dose was tested as a continuous covariate on $F$ but was not significant. The final model showed that weight, smoking status,

age and total bilirubin were predictors of CL/*F*, weight was a predictor of *V*/*F* and gender was a predictor of *F*. The correlation between CL/*F* and *V*/*F* was low (correlation = 0.375, %RSE = 33%) in the final model and removed (11 point increase in OFV).

The parameter estimates of the final PK model are presented in Table 3. The reference population was a 40-year-old, 70 kg male, non-current smoker, with total bilirubin of 9 μmol $l^{-1}$ administered >10 mg dose. The estimated typical (95% CI) parameter values were: CL/*F* = 0.901 (0.864, 0.938) l $h^{-1}$, *V*/*F* = 17.4 (16.5, 18.3) l, $k_a$ = 2.24 (1.56, 2.92) $h^{-1}$ and absorption $t_{lag}$ = 0.263 (0.0942, 0.432) h. There was a 35% increase in CL/*F* for study ING111521 compared with SPRING-1 and SPRING-2. There was a 24% increase in oral bioavailability for the 10 mg dose compared with the 25 and 50 mg doses. Apparent clearance of DTG was, on average, 16% (95% CI: 10%, 22%) higher in current smokers than non-current smokers. Oral bioavailability (*F*) was, on average, 21% (95% CI: 13%, 29%) higher in female subjects compared with males. Apparent clearance and volume of distribution increased with weight with a power coefficient of 0.438 and 0.768, respectively (i.e. as $(WT/70)^{0.438}$ and $(WT/70)^{0.768}$, respectively). For the range of weights in the analysis population (39–135 kg), CL/*F* ranged from 0.697–1.201 $h^{-1}$, which was 23% lower to 33% higher compared with a 70 kg subject and *V*/*F* ranged from 11.1–28.8 l, which was 36% lower to 66% higher compared with a 70 kg subject. Apparent clearance increased with age with a power coefficient of 0.193 (i.e. as $(AGE/40)^{0.193}$), and for the range of age in the analysis population (18–68 years), CL/*F* ranged from 0.772–0.998 l $h^{-1}$. Apparent clearance decreased with increasing total bilirubin with a power coefficient of −0.211 (i.e. as $(BILI/9)^{-0.211}$), and for the range of total bilirubin in the analysis population (3-38 μmol $l^{-1}$), CL/*F* ranged from 1.14-0.665 l $h^{-1}$. Race, ethnicity, HCV co-infection, CDC classification, albumin, CRCL, ALT or aspartate aminotransferase (AST) did not influence the PK of DTG in this analysis.

All of the fixed effect parameters were estimated with good precision (%RSE <24%) apart from absorption $t_{lag}$ (%RSE = 32.7%). The inter-individual random effects were also estimated with reasonable precision (%RSE <40%). IOV was tested in all PK parameters, of which an inclusion of IOV on CL/*F* was significant with a reduction of OFV by

## Table 3

Parameter estimates of final dolutegravir population PK model

| Parameter (units) | NONMEM estimates Point estimate | %RSE | 95% CI | | Bootstrap estimates* Median | 95% CI |
|---|---|---|---|---|---|---|
| **CL/*F* (l $h^{-1}$)†** | 0.901 | 2.11 | 0.864, 0.938 | | 0.901 | 0.866, 0.940 |
| ***V*/*F* (l)‡** | 17.4 | 2.49 | 16.5, 18.3 | | 17.4 | 16.6, 18.2 |
| **$k_a$ ($h^{-1}$)** | 2.24 | 15.4 | 1.56, 2.92 | | 2.21 | 1.73, 3.10 |
| **ALAG (h)** | 0.263 | 32.7 | 0.0942, 0.432 | | 0.262 | 0.0833, 0.393 |
| **CL/*F* ~ proof-of-concept** | 1.35 | 4.83 | 1.22, 1.48 | | 1.35 | 1.24, 1.51 |
| ***F* ~ 10 mg§** | 1.24 | 2.92 | 1.17, 1.31 | | 1.24 | 1.17, 1.31 |
| **CL/*F* ~ WT** | 0.438 | 16.9 | 0.293, 0.583 | | 0.440 | 0.290, 0.582 |
| ***V*/*F* ~ WT** | 0.768 | 10.8 | 0.605, 0.931 | | 0.774 | 0.616, 0.944 |
| ***F* ~ GENDER§** | 1.21 | 3.27 | 1.13, 1.29 | | 1.21 | 1.13, 1.30 |
| **CL ~ SMOKING** | 1.16 | 2.45 | 1.10, 1.22 | | 1.16 | 1.10, 1.22 |
| **CL ~ AGE** | 0.193 | 23.7 | 0.103, 0.283 | | 0.195 | 0.105, 0.283 |
| **CL ~ BILIRUBIN** | −0.211 | 14.0 | −0.269, −0.153 | | −0.212 | −0.267, −0.152 |
| **Inter-individual or inter-occasion variability** | | | | **CV%‖** | | |
| $\omega^2_{CL}$ | 0.0551 | 9.27 | 0.0451, 0.0651 | 23.5 | 0.0539 | 0.0449, 0.0652 |
| $\omega^2_{V}$ | 0.0188 | 29.5 | 0.00794, 0.0297 | 13.7 | 0.0182 | 0.00714, 0.0295 |
| $\omega^2_{ka}$ | 0.224 | 38.8 | 0.0535, 0.395 | 50.1 | 0.217 | 0.0613, 1.11 |
| $\omega^2_{IOV\text{-}CL}$ | 0.0296 | 15.6 | 0.0205, 0.0387 | 17.2 | 0.0300 | 0.0184, 0.0407 |
| **Residual variability** | | | | **CV%** | **Median** | **95% CI** |
| $\sigma^2_{prop}$ | 0.0704 | 7.41 | 0.0602, 0.0806 | 26.5 | 0.0698 | 0.0555, 0.0830 |

%RSE: percent relative standard error of the estimate = SE/parameter estimate × 100; 95% CI = 95% confidence interval on the parameter; ALAG, absorption lag-time; CL/*F*, apparent clearance; CV, coefficient of variation of proportional error (=$[\sigma^2_{prop}]^{0.5}$*100); IOV, inter-occasion variability; $k_a$, absorption rate constant; PK, pharmacokinetics; $\sigma^2_{prop}$, proportional component of the residual error model; *V*/*F*, volume of central compartment; $\omega^2_{CL}$, $\omega^2_{V}$, and $\omega^2_{ka}$, variance of random effect of CL/*F*, *V*/*F* and $k_a$, respectively.The reference population for PK parameters CL/*F* and *V*/*F* are 40-year-old, 70 kg male, non-current smoker, with total bilirubin of 9 μmol $l^{-1}$. *From 1000 completed bootstrap runs; †$CL/F = 0.901 \times 1.16^{SMOK} \times 1.35^{POC} \times (WT/70)^{0.438} \times (AGE/40)^{0.193} \times (BILI/9)^{-0.211}$ (SMOK = 1 for smoking subjects and = 0 for non-smoking subjects; POC = 1 for study ING111521 and = 0 for other studies); ‡$V/F = 17.4 \times (WT/70)^{0.768}$; §$F = 1.21^{GEND} \times 1.24^{DOSE}$ (GEND = 1 for females and = 0 for males; DOSE = 1 for 10 mg dose and = 0 for other doses) ‖ $CV_{TV_P} = \sqrt{e^{\omega^2_P} - 1}$ when $\omega^2_P$ exceeds 0.15

>100 points and good precision (%RSE = 15.6). As a result, IOV for CL/*F* (17.2%) was retained in the model.

The diagnostic plots for the final model (Figure 1) indicated that the model adequately described the data. The distributions of the random effects were close to normal, and they were not correlated. No strong unexplained covariate–parameter relationships were noticeable.

Figure 2 presents the results of the PC-VPC for the final model. The results of the PC-VPC indicate that the final PK model provided a good description of the data.

The bootstrap results were very similar to the NONMEM estimates from the final PK model (Table 3), supporting the stability of the population PK model and the good precision of NONMEM parameter estimates.

Steady-state AUC(0-τ), $C_{max}$, $t_{max}$ and $C_{\tau}$ of DTG were derived from the final model by an empirical Bayes estimation method (Table 4). Consistent with the final PK model, DTG exposure (AUC(0-τ) and $C_{max}$) was 20% to 50% lower in study ING111521 compared with the same doses in SPRING-1 (10 mg and 50 mg) and SPRING-2 (50 mg), which is in agreement with the 35% higher CL/*F* in study ING111521 as described by the final PK model. Dose-proportional PK were seen between the 25 and 50 mg doses. However, slightly higher than dose-proportional PK were observed at the 10 mg dose, in agreement with the model that the relative oral bioavailability of the 10 mg dose is approximately 24% higher than the 25 and 50 mg doses. The average $t_{max}$ was approximately 2 h across all studies and doses. For subjects receiving DTG 50 mg once daily in the three studies ($n$ = 449), the geometric mean (CV%) [5$^{th}$%, 95$^{th}$%] of estimated DTG AUC(0-τ), $C_{max}$ and $C_{\tau}$ were 53.6 μg ml$^{-1}$ h (26.9%) [35.1, 84.9 μg ml$^{-1}$ h], 3.67 μg ml$^{-1}$ (19.7%) [2.74, 5.19 μg ml$^{-1}$] and 1.11 μg ml$^{-1}$ (46.3%) [0.532, 2.24 μg ml$^{-1}$], respectively.

## Simulation

Forest plots for the comparison of steady-state DTG $C_{max}$, AUC(0-τ) and $C_{\tau}$ among various subpopulations are presented in Figure 3 to illustrate and confirm the PK model findings of covariate effect on DTG PK in terms of systemic exposure. On average, DTG $C_{max}$, AUC(0-τ) and $C_{\tau}$ were 32%, 26% and 15% higher in females, respectively.

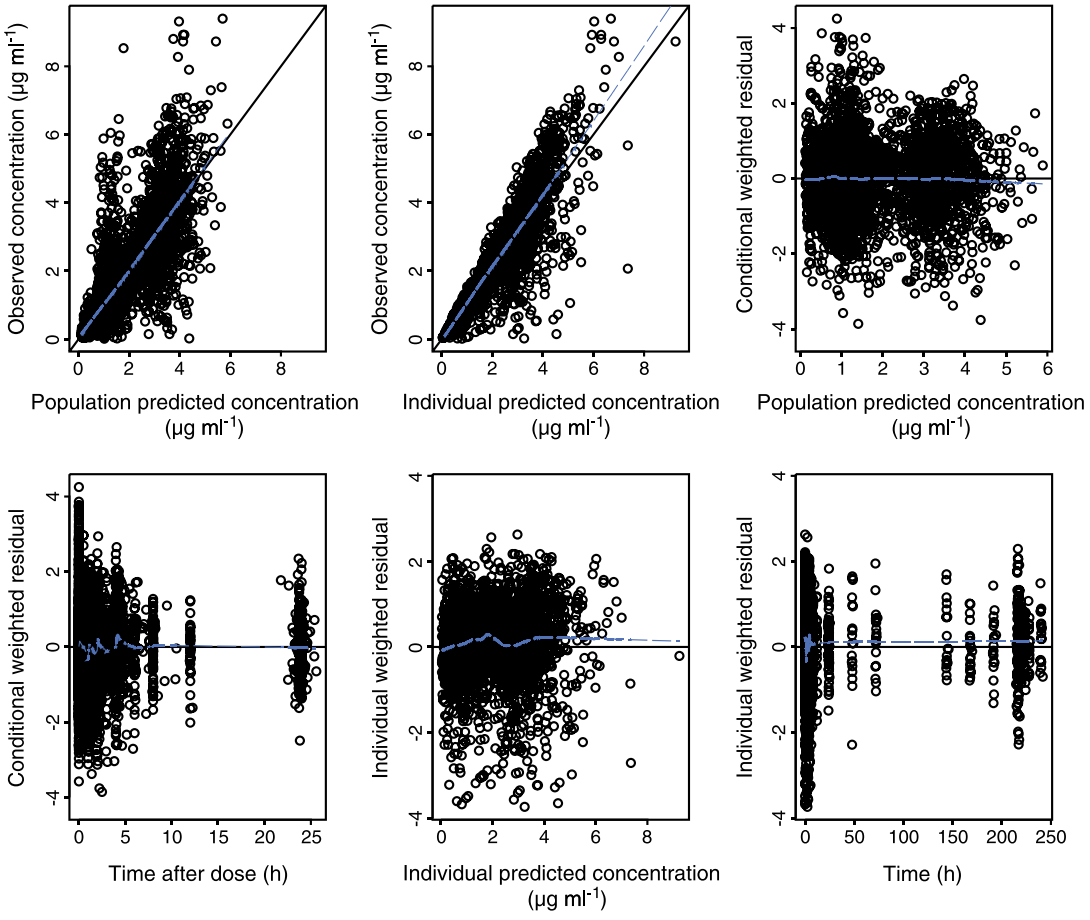


**Figure 1**

Goodness-of-fit and diagnostic plots. Each plot shows the line of unity (solid line) and Loess line (dashed line)

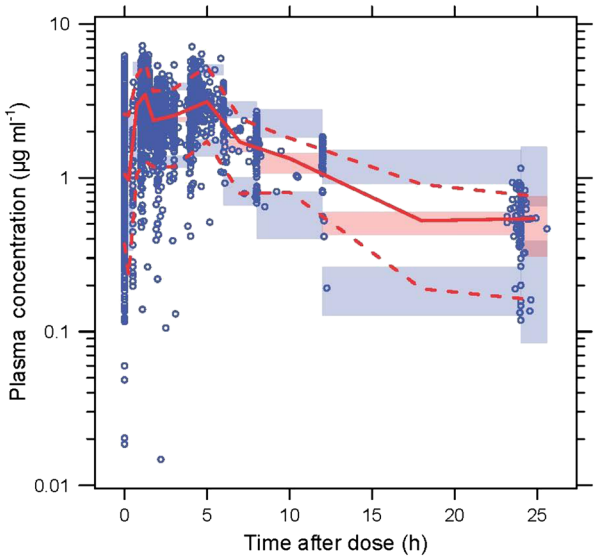


**Figure 2**

Prediction-corrected visual predictive check. Open circles: observed data, red lines: observed median (solid), 5th and 95th percentiles (dashed), shaded areas: 90% confidence intervals for median (red) 5th and 95th percentiles (blue) of simulated data

DTG $C_{max}$, AUC(0-τ) and $C_\tau$ were 7%, 13% and 22% lower in current smokers, respectively. Exposure decreased with increasing weight. For the weight groups (based on quartiles) 66–75 kg, 75–84 kg and >84 kg, $C_{max}$ was 14%, 20% and 28% lower, AUC(0-τ) was 12%, 17% and 24% lower and $C_\tau$ was 7%, 8% and 15% lower compared with the ≤66 kg group, respectively. Exposure decreased with increasing age. For elderly subjects >55 years, $C_{max}$, AUC(0-τ) and $C_\tau$ was 10%, 14% and 18% lower compared with subjects ≤55 years. Subjects with background therapy TDF/FTC had 6%, 5% and 4% lower $C_{max}$, AUC(0-τ) and $C_\tau$ than those with background therapy of ABC/3TC, respectively, which is of no clinical significance. For total bilirubin (based on quartiles), $C_{max}$, AUC(0-τ) and $C_\tau$ were comparable for the ≤7 and 7–9 μmol l$^{-1}$ groups. For the 9–12 and >12 μmol l$^{-1}$ groups, $C_{max}$ was 2% and 18% higher, AUC(0-τ) was 7% and 17% higher and $C_\tau$ was 17% and 38% higher, respectively, compared with the ≤7 μmol l$^{-1}$ group. Covariates HBV/HCV co-infection, race and ethnicity were not significant covariates in the models, and very little difference was found in $C_{max}$, AUC(0-τ) and $\boldsymbol{C}_\tau$ within these covariates.

### *Exploratory PK–PD relationship*

The PK–PD exploratory graphical analysis showed no relationship between any of the efficacy endpoints (antiviral response and CD4+ increase) and DTG exposure (steady-state AUC(0-τ), $C_{max}$ and $C_\tau$) in treatment-naive subjects. No relationship between DTG exposure and the safety endpoints was observed, except that serum creatinine (Figures 4 and 5) and CRCL (Figures 6 and 7) appeared to be slightly correlated with DTG exposure.

## Discussion

The PK of DTG were described by a linear one compartment model with absorption $t_{lag}$, first order absorption and elimination. Lower body weight, non-smoking status, lower age, higher total bilirubin at baseline and female gender were associated with higher plasma DTG exposure, either through effects on CL or *F*. The magnitude of effect of each covariate on CL or *F* was relatively

**Table 4**

Summary of steady-state $C_{max}$, $t_{max}$, $C_\tau$ and AUC(0-τ) following actual dose of dolutegravir administered in the studies

| Study | Dose (mg) | Statistic | AUC(0-τ) (μg ml$^{-1}$ h) | $C_{max}$ (μg ml$^{-1}$) | $t_{max}$ (h) | $C_\tau$ (μg ml$^{-1}$) |
|---|---|---|---|---|---|---|
| **ING111521** | **10** | ***n**** | 9 | 9 | 9 | 9 |
| | | **Geometric mean (95% CI)** | 9.33 (8.16, 10.7) | 0.691 (0.606, 0.788) | 1.66 (1.17, 2.35) | 0.168 (0.136, 0.208) |
| | **50** | ***n*** | 10 | 10 | 10 | 10 |
| | | **Geometric mean (95% CI)** | 41.3 (38.4, 44.4) | 2.94 (2.65, 3.27) | 1.94 (1.65, 2.29) | 0.785 (0.689, 0.895) |
| **SPRING-1** | **10** | ***n*** | 49 | 49 | 49 | 49 |
| | | **Geometric mean (95% CI)** | 14.3 (13.4, 15.3) | 0.957 (0.908, 1.01) | 2.00 (2.00, 2.00) | 0.311 (0.281, 0.345) |
| | **25** | ***n*** | 46 | 46 | 46 | 46 |
| | | **Geometric mean (95% CI)** | 25.7 (23.6, 28.1) | 1.77 (1.66, 1.89) | 2.00 (2.00, 2.00) | 0.530 (0.462, 0.609) |
| | **50** | ***n*** | 46 | 46 | 46 | 46 |
| | | **Geometric mean (95% CI)** | 53.8 (49.6, 58.2) | 3.58 (3.37, 3.80) | 2.00 (2.00, 2.00) | 1.17 (1.04, 1.33) |
| **SPRING-2** | **50** | ***n*** | 403 | 403 | 403 | 403 |
| | | **Geometric mean (95% CI)** | 53.6 (52.3, 55.0) | 3.69 (3.62, 3.76) | 2.00 (2.00, 2.00) | 1.10 (1.05, 1.15) |

AUC(0-τ), steady state area under the plasma concentration–time curve over the dosing interval (τ); CI, confidence interval; $C_{max}$, maximum plasma concentration at steady-state; $C_\tau$, concentration at time τ; $t_{max}$, time to $C_{max}$.*95% CI = 95% confidence interval for geometric mean.

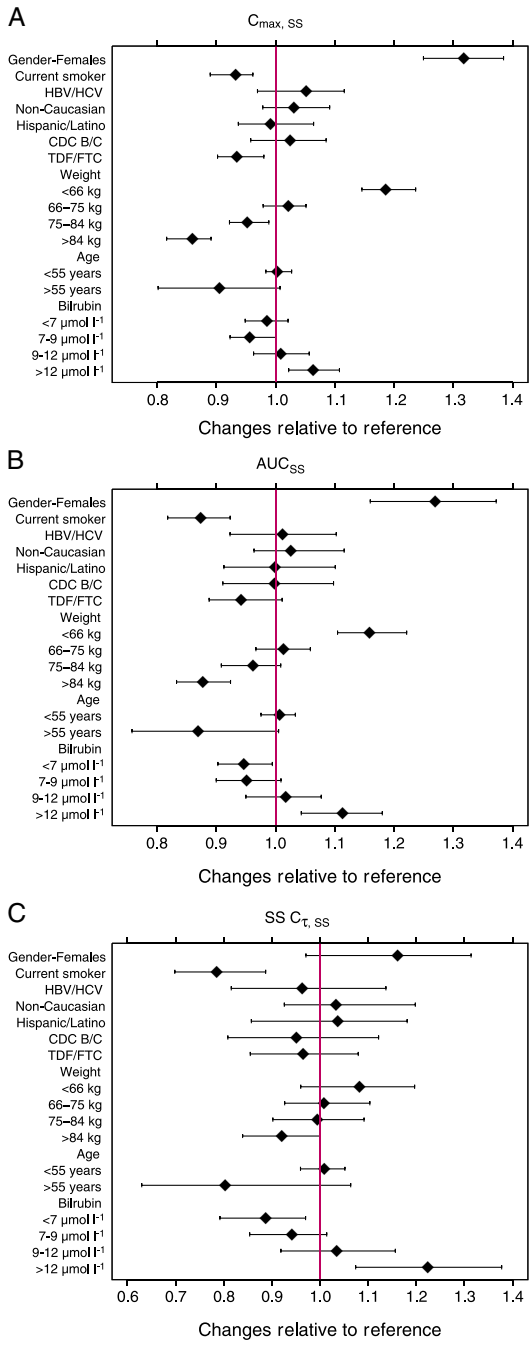


## Figure 3

Predicted fold change in steady-state (**A**) $C_{max}$, (**B**) AUC(0-τ) and (**C**) $C_{\tau}$ of dolutegravir relative to reference covariate category (fold change in median and 90% confidence interval). Reference categories: male, non-current smoker, no HBV/HCV co-infection, Caucasian, non-Hispanic/Latino, CDC A, ABC/3TC for gender, smoking status, HBV/HCV co-infection, race, ethnicity, CDC, and background therapy, respectively. For continuous covariates, the overall median was used to normalize the $C_{max}$, AUC(0-τ) and $C_{\tau}$ of each category (i.e., 4.43 μg ml$^{-1}$, 52.8 μg ml$^{-1}$ h, and 1.12 μg ml$^{-1}$ for $C_{max}$, AUC(0-τ) and $C_{\tau}$, respectively). ABC/3TC, abacavir/lamivudine; AUC(0-τ), steady-state area under the plasma concentration–time curve over the dosing interval (τ); CDC, Centres for Disease Control and Prevention; $C_{max}$, maximum plasma concentration at steady-state; $C_{\tau}$, concentration at time τ; HBV, hepatitis B virus; HCV, hepatitis C virus; ss, steady state; TDF/FTC, tenofovir disoproxil fumarate/emtricitabine

small (all less than 30%, Table 3), and the magnitude of effect on steady-state AUC(0-τ), $C_{max}$ and $C_{\tau}$ of DTG was <32% (Figure 3). Based on the known safety profile and PK/PD relationships for the antiviral activity of DTG, the likely range of DTG therapeutic effect encompasses these changes. Subgroup analysis on week 48 antiviral response in SPRING-2 demonstrated that there were no effects of gender and age on response [17]. Thus, the effects of these covariates are not considered clinically significant. Therefore, no DTG dose adjustment by these covariates is necessary.

The final PK model indicated that mean (95% CI) CL/*F* was 16% (10%, 22%) higher in current smokers compared with non-smokers/former smokers. DTG is metabolized primarily by UGT1A1 with CYP3A4 as a secondary pathway. Tobacco smoking has been shown to induce hepatic CYP isozymes including 1A1, 1A2, 2B6, 3A4 and possibly 2E1 [18–22], and it may also have the potential to induce UGT1A1 activity [22, 23]. The reason for the higher CL/*F* of DTG seen in current smokers in this analysis may be related to the enzyme induction effect of tobacco smoking.

The final PK model also indicated that there was a 21% (13%, 29%) increase in mean (95% CI) oral bioavailability in women compared with men. DTG is a known substrate of drug transporters Pgp and BCRP. It has been suggested [24] that gender may play a role in the expression of drug transporters, which could influence the drug disposition and may partly explain gender differences in oral bioavailability. Nevertheless, the actual mechanism that contributed to the gender difference in oral bioavailability of DTG merits further investigation.

Apparent clearance unexpectedly increased with age with a positive power coefficient of 0.193 (95% CI: 0.103, 0.283) (i.e. as $(AGE/40)^{0.193}$). Clearance is often lower in elderly people. The reason for the unexpected effect of age on DTG CL/*F* may be associated with decreased absorption of DTG with age. For highly protein bound molecules like DTG, reduction in protein binding capacity and decrease in plasma albumin concentrations, as commonly seen in the elderly, may have contributed to the increased CL/*F* with age [25]. In the current analysis, age was slightly but inversely correlated with baseline albumin. However, age in the model had a lower OFV than baseline albumin in the model, suggesting that the increase in CL/*F* with age cannot be fully attributed to the decrease in plasma albumin concentrations. Since the data in elderly subjects were limited in the current analysis (17 [3%] aged >55 years and 1 aged >65 years), additional data from elderly subjects may be warranted to understand further the PK of DTG in this population.

Apparent clearance also decreased with total bilirubin with a negative power coefficient of −0.211 (95% CI: −0.269, −0.153). For the range of total bilirubin in the analysis

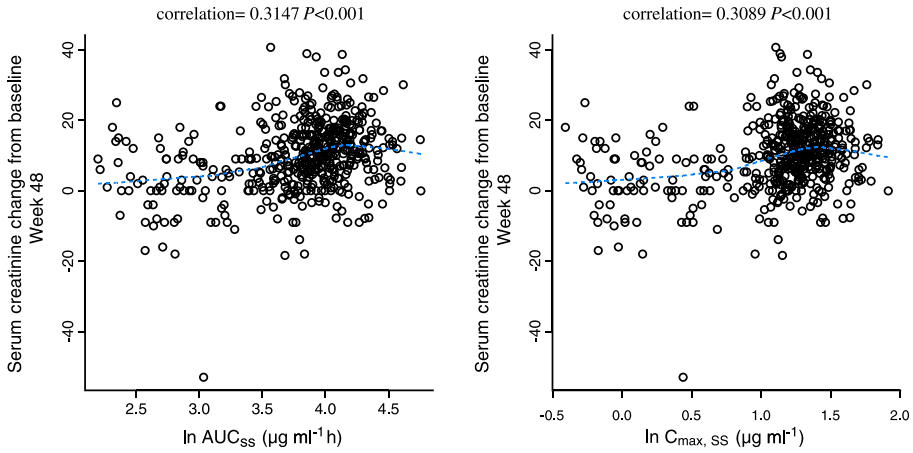


**Figure 4**

Serum creatinine change from baseline at week 48 *vs*. dolutegravir exposure ($C_{max}$ and AUC(0-τ))-SPRING-1 and SPRING-2. Each plot shows the individual observed data (open circle) and the Loess line (dashed line). AUC(0,τ), steady-state area under the plasma concentration–time curve over the dosing interval (τ); $C_{max}$, maximum plasma concentration at steady-state; ss, steady-state

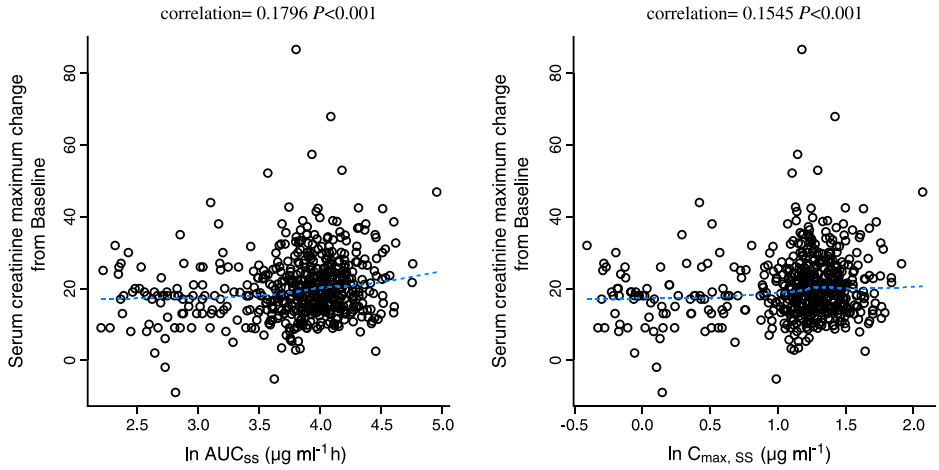


**Figure 5**

Serum creatinine maximum change from baseline *vs*. dolutegravir exposure ($C_{max}$ and AUC(0-τ))-SPRING-1 and SPRING-2. Each plot shows the individual observed data (open circle) and the Loess line (dashed line). AUC(0-τ), steady-state area under the plasma concentration–time curve over the dosing interval (τ); $C_{max}$, maximum plasma concentration at steady state; ss, steady state

(3–38 μmol $l^{-1}$), CL/*F* would range from 26% higher to 26% lower compared with a subject with total bilirubin of 9 μmol $l^{-1}$. The relationship between DTG CL/*F* and total bilirubin is likely attributable to competition between DTG and bilirubin for the same metabolic pathway (UGT1A1).

There was a 35% higher CL/*F* for study ING111521 compared with the other two studies. The reason behind such a study difference is not fully understood. There may be factors in these studies that are not accounted for with the available covariates to explain this difference. Although study ING111521 was a DTG monotherapy study, and SPRING-1 and SPRING-2 were combination treatment studies, no difference in DTG PK was expected between subjects receiving monotherapy *vs*. combination therapy with ABC/3TC or TDF/FTC, as these NRTIs do not share and have no effect on the elimination pathways of DTG (UGT1A1 and CYP3A). A smaller sample size and thus less diverse patient population in study ING111521 *vs*. SPRING-1 and SPRING-2 may potentially account for the difference in the estimated CL/*F* between these studies.

There was a difference in bioavailability by dose, 24% higher bioavailability for the 10 mg dose compared with the 25 and 50 mg doses. Dose as a continuous covariate was investigated but was not significant, and no difference was found when separate bioavailability was estimated for the 25 mg dose compared with the 50 mg dose. The reason for a higher oral bioavailability at the lower dose is possibly due to better dispersion of the tablet at lower tablet strength.

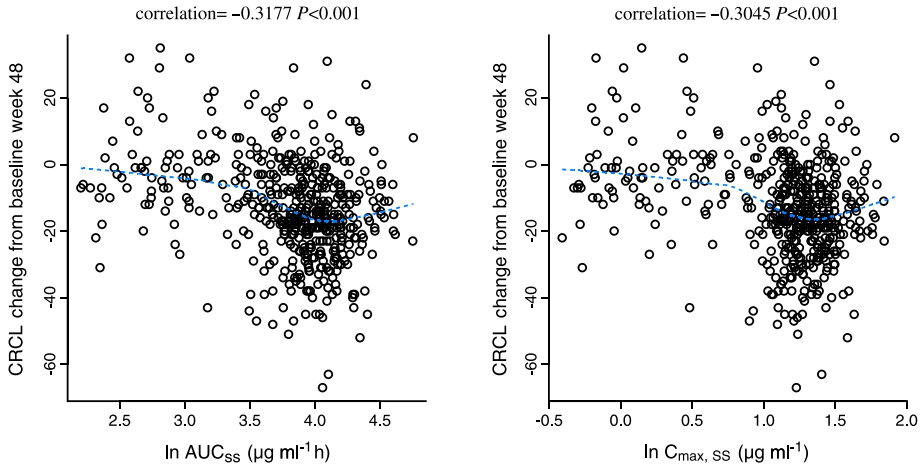


**Figure 6**

Creatinine clearance change from baseline at week 48 *vs*. dolutegravir exposure ($C_{max}$ and AUC(0-τ))-SPRING-1 and SPRING-2. Each plot shows the individual observed data (open circle) and the Loess line (dashed line). AUC(0-τ), steady state area under the plasma concentration–time curve over the dosing interval (τ); $C_{max}$, maximum plasma concentration at steady state; $CL_{cr}$, creatinine clearance; ss, steady-state

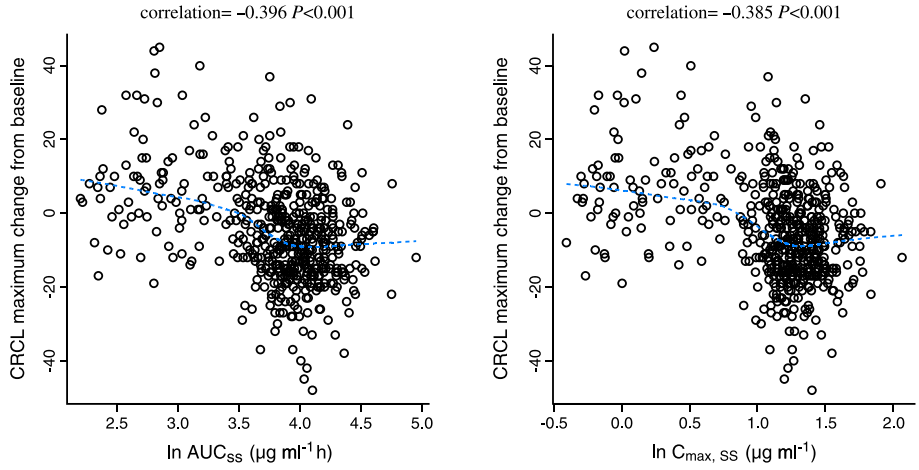


**Figure 7**

Creatinine clearance maximum change from baseline *vs*. dolutegravir exposure ($C_{max}$ and AUC(0-τ))-SPRING-1 and SPRING-2. Each plot shows the individual observed data (open circle) and the Loess line (dashed line). AUC(0-τ), steady-state area under the plasma concentration–time curve over the dosing interval (τ); $C_{max}$, maximum plasma concentration at steady-state; $CL_{cr}$, creatinine clearance; ss, steady-state

IOV was assessed in the model which improved individual predictions. The estimated IOV on CL/*F* was 17%, which is quite similar to the estimated intra-subject variability based on phase 1 studies in healthy adult subjects. The IOV is probably due to variation in absorption, although day-to-day variability in metabolic enzyme activity (such as UGT1A1 or CYP3A4) may also contribute to the estimated IOV. Compared with the residual variability estimated from this analysis (26.5%), the magnitude of IOV is not considered significant and therefore of little clinical relevance. This also provided the reasonable justification for not including IOV in simulation, given the main focus of simulation in this analysis was the central tendency of DTG exposure among various subpopulations.

DTG PK were similar between healthy and HIV-1 infected subjects. Based on analysis using pooled PK data following DTG 50 mg once daily (fasted and fed) in phase 1 studies, geometric means (CV%) of DTG AUC(0-τ), $C_{max}$ and $C_{\tau}$ were estimated at 49.1 μg ml$^{-1}$ h (41%), 3.62 μg ml$^{-1}$ (35%) and 1.05 μg ml$^{-1}$ (56%), respectively (internal data). These values were comparable with those presented in Table 4 based on the population PK analysis.

The PK–PD exploratory graphical analysis showed no relationship between any of the efficacy endpoints (antiviral response and CD4+ increase) and DTG exposure (steady-state AUC(0-τ), $C_{max}$ and $C_{\tau}$) in treatment-naive subjects, which is likely due to the high potency

of the combination of DTG at 10 to 50 mg once daily with two active NRTIs. The lack of PK/PD relationship also indicates that the antiviral effect of DTG (when in combination with two active NRTIs) is at maximum at doses of 10 mg once daily or higher. No relationship between DTG exposure (AUC(0-τ), $C_{max}$ and $C_{\tau}$) and the safety endpoints was observed, except for serum creatinine and CRCL, which appeared to be correlated with DTG exposure. DTG is known to inhibit organic cation transporter, OCT2, which mediates the tubular secretion of creatinine in the proximal renal tubules [26]. The observed correlation between DTG exposure and serum creatinine/CRCL would be an expected finding based on OCT2 inhibition by DTG. However, given the magnitude of changes in these safety parameters, none of them was considered to be clinically significant, and therefore DTG dose adjustment by patient characteristics is not necessary in HIV-infected treatment-naive adult patients.

## Competing Interests

All authors have completed the Unified Competing Interest form at www.icmje.org/coi_disclosure.pdf (available on request from the corresponding author) and declare the submitted work was supported by ViiV Healthcare, JZ, IM, SP, SM and IS are employees of GlaxoSmithKline and hold stock options and SH and BS are employees of ICON. There are no other relationships or activities that could appear to have influenced the submitted work.

*Funding for this work was provided by ViiV Healthcare. All listed authors meet the criteria for authorship set forth by the International Committee for Medical Journal Editors. The authors attest that the funding source did not have an influence on the analysis and reporting of results. The authors wish to acknowledge the following individual for editorial assistance during the development of this manuscript: Jian Zong.*

## Contributors

Ivy H. Song designed and reviewed the analysis and prepared the manuscript. Jianping Zhang reviewed the data quality and analysis and prepared the manuscript. Siobhán Hayes and Brian Sadler performed the analysis and prepared the manuscript. Ilisse Minto oversaw the data quality and reviewed the manuscript. Steve Piscitelli and Sherene Min were involved in the design of the clinical studies in which PK data used in this analysis were generated, and reviewed and contributed to interpretation of the analysis and development of the manuscript.

## PI statement

None of the authors is the principal investigator as this manuscript presents results from a meta-analysis using pooled pharmacokinetic data from multiple studies.

## REFERENCES

1 Tivicay. [package insert]. Research Triangle Park, NC: ViiV Healthcare; 2014.

2 Tivicay. [summary of product characteristics]. Middlesex, UK: ViiV Healthcare UK Ltd; 2013.

3 Raffi F, Rachlis A, Stellbrink HJ, Hardy WD, Torti C, Orkin C, Bloch M, Podzamczer D, Pokrovsky V, Pulido F, Almond S, Margolis D, Brennan C, Min S; for the SPRING-2 Study Group. Once-daily dolutegravir versus raltegravir in antiretroviral-naive adults with HIV-1 infection: 48 week results from the randomised, double-blind, non-inferiority SPRING-2 study. Lancet 2013; 381: 735–43.

4 Cahn P, Pozniak AL, Mingrone H, Shuldyakov A, Brites C, Andrade-Villanueva JF, Richmond G, Buendia CB, Fourie J, Ramgopal M, Hagins D, Felizarta F, Madruga J, Reuter T, Newman T, Small CB, Lombaard J, Grinsztejn B, Dorey D, Underwood M, Griffith S, Min S, for the extended SAILING Study Team. Dolutegravir versus raltegravir in antiretroviral-experienced, integrase-inhibitor-naive adults with HIV: week 48 results from the randomised, double-blind, non-inferiority SAILING study. Lancet 2013; 382: 700–8.

5 Kobayashi M, Yoshinaga T, Seki T, Wakasa-Morimoto C, Brown KW, Ferris R, Foster SA, Hazen RJ, Miki S, Suyama-Kagitani A, Kawauchi-Miki S, Taishi T, Kawasuji T, Johns BA, Underwood MR, Garvey EP, Sato, A, Fujiwara T. *In vitro* antiviral properties of S/GSK1349572, a next-generation HIV integrase inhibitor. Antimicrob Agents Chemother 2011; 55: 813–21.

6 Castagna A, Maggiolo F, Penco G, Wright D, Mills A, Grossberg R, Molina JM, Chas J, Durant J, Moreno S, Doroana M, Ait-Khaled M, Huang J, Min S, Song I, Vavro C, Nichols G, Yeo JM, for the VIKING-3 Study Group. Dolutegravir in antiretroviral-experienced patients with raltegravir- and/or elvitegravir-resistant HIV-1: 24-week results of the phase III VIKING-3 study. J Infect Dis 2014; 210: 354–62.

7 Min S, Sloan L, DeJesus E, Hawkins T, McCurdy L, Song I, Stroder R, Chen S, Underwood M, Fujiwara T, Piscitelli S, Lalezari J. Antiviral activity, safety, and pharmacokinetics/pharmacodynamics of dolutegravir as 10-day monotherapy in HIV-1-infected adults. AIDS 2011; 25: 1737–45.

8 van Lunzen J, Maggiolo F, Arribas JR, Rakhmanova A, Yeni P, Young B, Rockstroh JK, Almond S, Song I, Brothers C, Min S. Once daily dolutegravir (S/GSK1349572) in combination therapy in antiretroviral-naive adults with HIV: planned interim 48 week results from SPRING-1, a dose-ranging, randomised, phase 2b trial. Lancet Infects Dis 2012; 12: 111–8.

9 Bennetto-Hood C, Tabolt G, Savina P, Acosta EP. A sensitive HPLC–MS/MS method for the determination of dolutegravir

in human plasma. J Chromatogr B Analyt Technol Biomed Life Sci 2014; 945-946: 225–32.

**10** Beal SL, Sheiner LB, Boeckmann AJ, Bauer RJ, eds. NONMEM user's guides (1989-2009). Ellicott City, MD: Icon Development Solutions, 2009.

**11** Gastonguay MR. Full covariate models as an alternative to methods relying on statistical significance for inferences about covariate effects: a review of methodology and 42 case studies. Abstract presented at: Population Approach Group Europe 20: 2011 June 7–10; Athens, Greece.

**12** Harrell FE. Regression modeling strategies: with applications to linear models, logistic regression, and survival analysis. 1st ed. New York: Springer-Verlag, 2001.

**13** Bergstrand M, Hooker AC, Wallin JE, Karlsson MO. Prediction-corrected visual predictive checks for diagnosing nonlinear mixed-effects models. AAPS J 2011; 13: 143–51.

**14** Lewis S, Clarke M. Forest plots: trying to see the wood and the trees. BMJ 2001; 322: 1479–80.

**15** Tan SH, Cooper NJ, Bujkiewicz S, Welton NJ, Caldwell DM, Sutton AJ. Novel presentational approaches were developed for reporting network meta-analysis. J Clin Epidemiol 2014; 67: 672–80.

**16** Hu C, Zhang J, Zhou H. Confirmatory analysis for phase III population pharmacokinetics. Pharm Stat 2011; 10: 14–26.

**17** Brinson C, Walmsley S, Arasteh K, Górgolas M, Schneider L, Brennan C, Pappa K, Almond S, Granier C, Raffi F. Dolutegravir treatment response and safety by key subgroups in treatment naive HIV infected individuals. Poster session presented at: 20th Conference on Retroviruses and Opportunistic Infections; 2013 March 3–6; Atlanta, GA.

**18** Zhou SF, Yang LP, Zhou ZW, Liu YH, Chan E. Insights into the substrate specificity, inhibitors, regulation, and polymorphisms and the clinical impact of human cytochrome P450 1A2. AAPS J 2009; 11: 481–94.

**19** Washio I, Maeda M, Sugiura C, Shiga R, Yoshida M, Nonen S, Fujio Y, Azuma J. Cigarette smoke extract induces CYP2B6 through constitutive androstane receptor in hepatocytes. Drug Metab Dispos 2011; 39: 1–3.

**20** Schaffer SD, Yoon S, Zadezensky I. A review of smoking cessation: potentially risky effects on prescribed medications. J Clin Nurs 2009; 18: 1533–40.

**21** Hamilton M, Wolf JL, Rusk J, Beard SE, Clark GM, Witt K, Cagnoni PJ. Effects of smoking on the pharmacokinetics of erlotinib. Clin Cancer Res 2006; 12: 2166–71.

**22** Zevin S, Benowitz NL. Drug interactions with tobacco smoking. An update Clin Pharmacokinet 1999; 36: 425–38.

**23** van der Bol JM, Mathijssen RH, Loos WJ, Friberg LE, van Schaik RH, de Jonge MJ, Planting AS, Verweij J, Sparreboom A, de Jong FA. Cigarette smoking and irinotecan treatment: pharmacokinetic interaction and effects on neutropenia. J Clin Oncol 2007; 25: 2719–26.

**24** Ofotokun I. Sex differences in the pharmacologic effects of antiretroviral drugs: potential roles of drug transporters and phase 1 and 2 metabolizing enzymes. Top HIV Med 2005; 13: 79–83.

**25** Hayes MJ, Langman MJ, Short AH. Changes in drug metabolism with increasing age: 2. Phenytoin clearance and protein binding. Br J Clin Pharmacol 1975; 2: 73–9.

**26** Urakami Y, Kimura N, Okuda M, Inui K. Creatinine transport by basolateral organic cation transporter hOCT2 in the human kidney. Pharm Res 2004; 21: 976–81.